October 1, 2006

For *Macromolecules*

Supporting Information

Matrix Fluorescence Photobleaching Recovery for Polymer Molecular Weight Distributions and Other Applications

G. J. Doucet, D. Dorman, R. Cueto, D. Neau, P. S. Russo*

Department of Chemistry and Macromolecular Studies Group

Louisiana State University, Baton Rouge, LA 70803, USA

D. De Kee

Department of Chemical Engineering

Tulane University, New Orleans, LA 70118 USA

J. Pople, Stanford Synchrotron Radiation Laboratory

Stanford Linear Accelerator Center Stanford, CA 94309 USA

To whom correspondence should be addressed: chruss@lsu.edu

Instrument Details. Some modifications have occurred since the FPR setup was described.[1-5] Briefly, a beam with λ = 488 nm (supplied by a Lexel Model 3000 or Lexel Model 95 Argon Ion Laser) passes through an acousto-optic modulator (Newport Electro-Optical Systems Model N35085-3) splitting the laser output in two beams, one being dim (weak) and the other being bright (strong). The weak beam excites the fluorophores in the detection part of the experiment while the bright beam photobleaches the sample. The beam bounces off two mirrors through a Ronchi ruling (a 1″ X 1″ glass with equal clear and black stripes, Edmund Industrial Optics) entering the rear focal plane of an Olympus BHA microscope. The Ronchi ruling is mounted on a speaker system made from two opposing 4″ woofers (Radio Shack catalog number 40-1022B) controlled by a LSU-built driver to create the vibrations at a chosen frequency for measurement. The beam reflects off a dichroic mirror down to the sample through an objective. The labeled polymers in the sample fluoresce, and what is seen when looking at the sample is a striped pattern from the Ronchi ruling. The fluorescent light, λ = 515 nm, passes through the dichroic mirror, a shutter (Newport Industrial Optics controlled with a LSU built driver) and through a filter set to the fluorescing light into a photomultiplier tube (RCA-7265 powered by a Hewlett-Packard 6515A DC Power Supply). The signal generated by the PMT is fed into a Stanford Research Systems Model SR560 Low Noise Preamplifier then into a tuned amplifier built in the LSU electronics shop. A Tektronix 221A 100 MHz Digital Storage Oscilloscope monitors the sinusoidal (actually, triangular just after the photobleaching) wave generated in the experiment and runs parallel with the amplifier. The signal from the amplifier is transmitted to an analog-digital card from National Instruments, #AT-MIO-16D Part #320489-01 then into a program to collect the sine wave amplitude. The program controls the switching of the AOM, shutter, and time the signal is collected.

Simulation Details. In Fig. S1 there appears a series of results, wherein polymers of different simulated molecular weights are cleanly identified from a sample at M = 10000. This suggests that good "separations" might be achieved over a very wide range of polymers. Figure S2 demonstrates that 10000 and 20000 molar mass samples can be cleanly identified, even though simulated with slightly more noise than was present in the decay profiles generated to produce Fig. S1, if one of the alternate (not chosen) solutions from CONTIN is selected. The essentially perfect response of a fit to two discrete exponential terms (vertical lines) is shown in order to drive home the point that Laplace inversion always leads to a certain amount of "band broadening." A perfectly monodisperse sample may be characterized as paucidisperse, with a polydispersity index, M_w/M_n, exceeding unity. A typical polydispersity index for the CONTIN-chosen solution would be < 1.05. This is not a practical problem for all but very detailed characterizations. A small peak, with large attendant noise, is evident at about M = 1500. This often appears in real analyses, too, and may be eliminated by not including some of the first data points in the recovery.

Figure S3 demonstrates that accurate results can be obtained from asymmetric bimodal distributions—i.e., those in which the fluorescent signal from the two components is not equal in amplitude. The leftmost data points represent the case where the fluorescent amplitude associated with polymer having M = 40000 is one-seventh as large as that associated with polymer at M = 80000. The amplitudes—i.e., fluorescent concentrations—are cleanly estimated regardless of the ratio of polymer concentrations simulated. Errors in molecular weight do become significant for very unbalanced distributions.

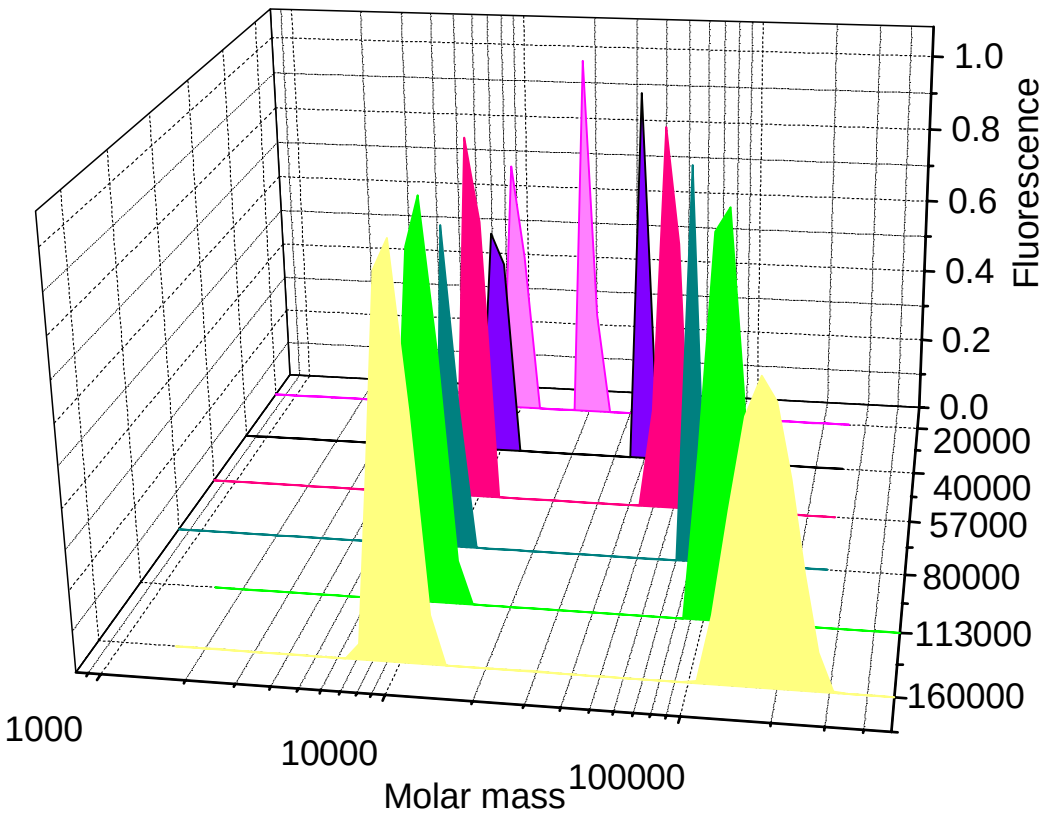

Figure S1. Resolution of diffusing components in simulated bimodal solutions, each with a component at *M*=10000. Other components are at *M*=20000, 40000, 57000, 80000, 113000 and 160000 as shown. The distributions have been normalized to unity at the highest grid point for the distributions automatically chosen by CONTIN.

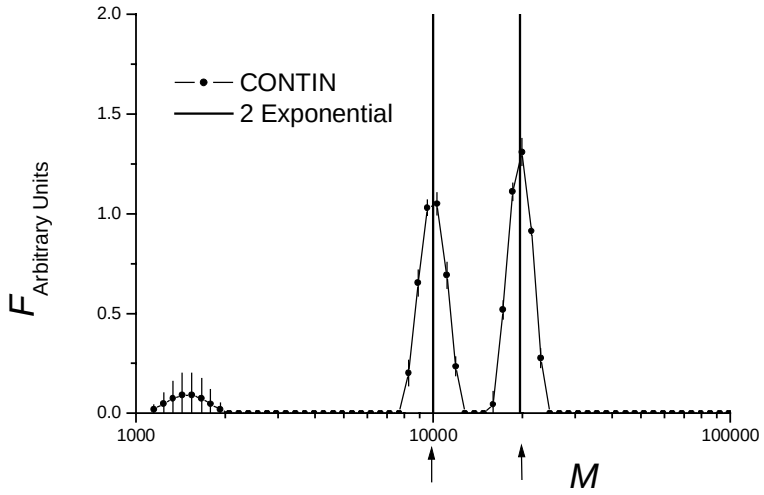

Figure S2. CONTIN-resolved distribution for simulated M = 10000 and M = 20000 (indicated with arrows) with comparison to double-exponential nonlinear least squares fitting analysis (vertical lines).

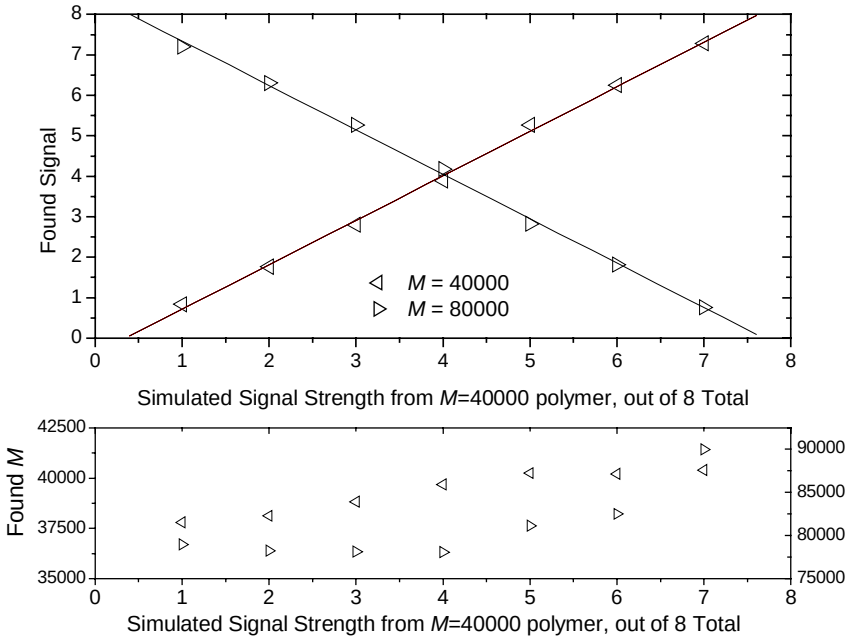

Figure S3. Top: CONTIN-found amplitudes associated with M = 40000 signal (ϖ) and M = 80000 signal (ω) as a function of simulated mode amplitudes. Bottom: CONTIN-found molecular weights corresponding to simulated M = 40000 signal (ϖ) and M = 80000

signal(ω).

Signal characteristics

Figure S4 displays a typical signal trace for a fluorescent pullulan (FP) sample, just as it is presented by the ANSCAN software during measurement. As shown by the calculated curve and residuals, the recovery is well fit by a single exponential (1EXP) algorithm with floating baseline, decay rate and initial amplitude. Recoveries for fluorescently labeled dextran (FD) tended to contain a fast-decaying component, which was judged to arise from free dye and small fragments because the FD samples were used as purchased, without purification. This is evident from Figure 5 in which the ILT from CONTIN appears simultaneously with the data, along with a vertical stripe to indicate the decay rate from 1EXP fitting. Despite the fast decay mode for FD samples, the average decay rate (hence, diffusion) from ILT agrees with the 1EXP result, rendering calibration curves built from either method equal. In the more uniform FP samples, sometimes a fast decay mode associated with noise was observed. It is not attributed to free dye, because labeling and purification was done in-house for the FP samples. Instead, this fast mode is attributed to spurious noise, and the associated amplitude errors are very large.

As practiced in this work, FPR is a single-shot method; while measurements were repeated, neither sum nor average of the raw data was computed. The point-by-point error bars associated with the FPR signals in Figures S4 and S5 are estimated by an algorithm that takes the data into semilogarithmic form and performs a linear fit to clusters of data to evaluate outliers. So estimated, the uncertainties are higher than often encountered using DLS or DOSY NMR, techniques that easily allow for extended data acquisition. It is apparent from the main text that the data are sufficiently quiet, and that run-by-run repeats permit realistic uncertainties for the mass distribution, including the ILT analysis which is an ill-conditioned problem.[6;7]

The precision on the diffusion coefficients is good. Daily measurements of FD-70 in dilute solution over a period of two weeks revealed a precision of about 2% and no trend, whether analyzed by 1EXP or CONTIN.

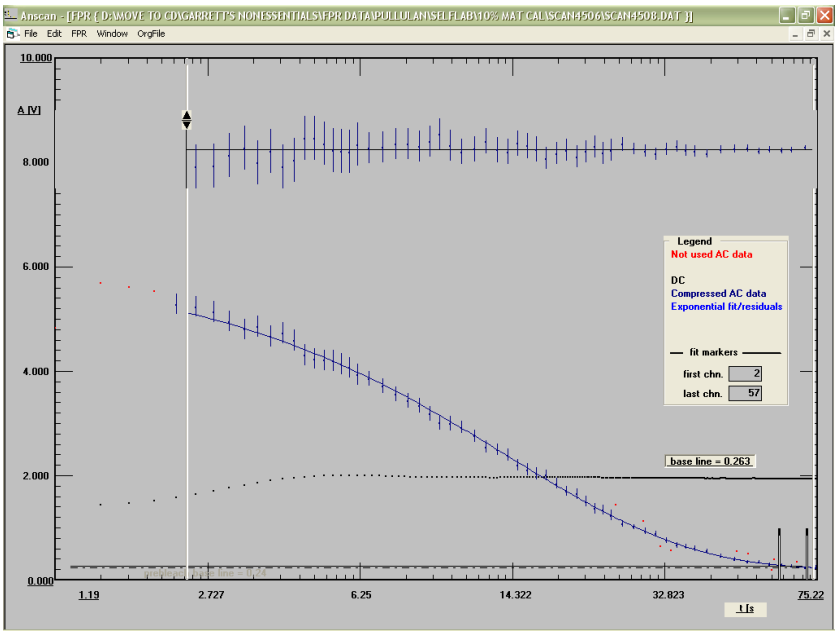

Figure S4. FP11.8 (Ronchi Ruling = 100 lines per inch; objective = 7X; K = 505.0 cm^{-1}; bleach for one second) diffusing through a w = 0.10 dextran matrix. The blue fitted line is the first order exponential decay fit of the data with the residuals shown above the curve.

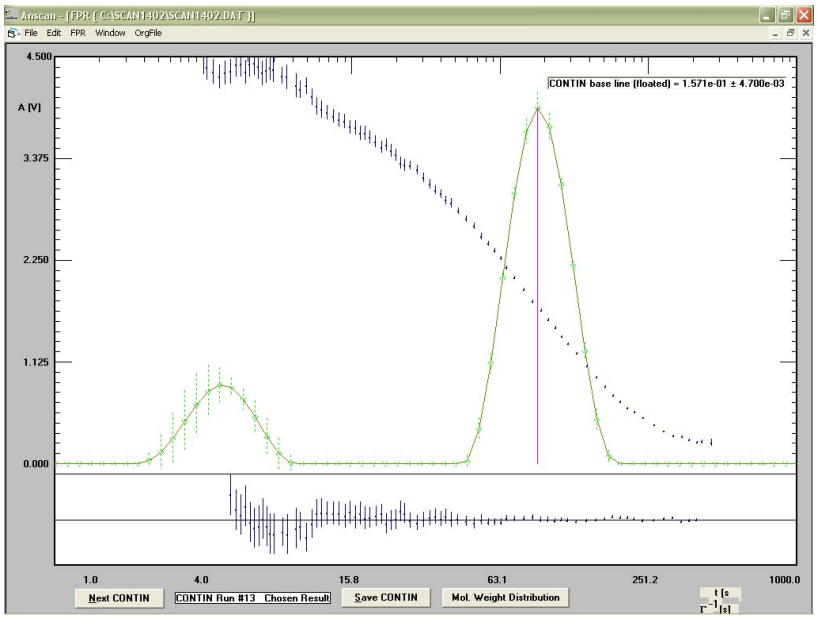

Figure S5. Illustration of the ILT overlay with the compressed data of FD10s diffusing through a w = 0.10 dextran matrix. The distribution is the ILT calculated amplitudes for inverse decay rates (indicated by Γ^{-1}). The vertical line indicates the value of Γ^{-1} from the 1EXP analysis; the residuals at the bottom are from the ILT fit and are bracketed by the experimental noise.

GPC-MALS Measurements of Dextran

As shown in Figure S6, we are unable to measure R_g vs M behavior reliably until M exceeds about 200,000. Over a range of almost one decade, FD500S gives a scaling exponent reminiscent of a slightly branched material. The high-M dextran we chose for matrix gives clear signs of "densifying" with molecular weight (alternately, the GPC resolution may be poor for this polymer).

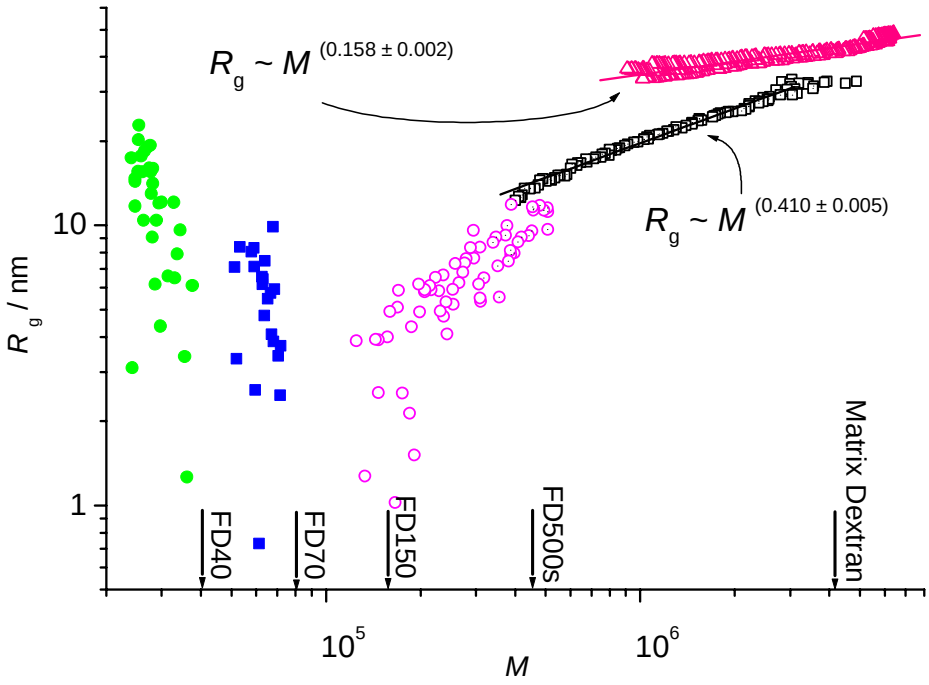

Figure S6. Representative radius of gyration versus molecular weight. From left to right: solid green circles, FD40; solid blue squares, FD70; magenta open circles, FD150, black open squares, FD500s; pink open triangles, dextran matrix. The lines through the data are linear fits. The downgoing arrows indicate M_w of the samples included. Scaling laws are indicated for FD500s and the dextran matrix.

Figure S7 shows the *c* vs. *M* distribution from GPC-MALS of two dextrans very similar in mass to the labeled dextrans that are the subject of Fig. 5 of the main text. Runs are displayed for each dextran separately and for the mixture, and conditions are given in the legend.

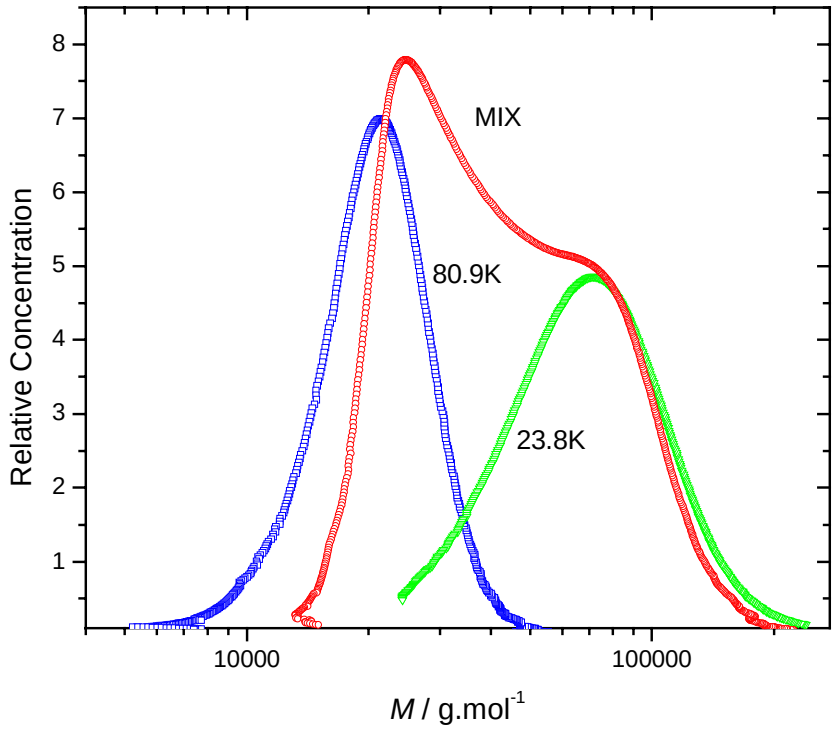

Figure S7. GPC-MALS separation of two mixed dextrans (*M* = 80.9K and 23.8K from Polymer Standard Services, Mainz, Germany). Also shown is the output of individual runs. Measured using Wyatt Heleos. Conditions: 23.8K (4.34 mg/ml); 80.9K (4.32 mg/ml); Mix(4.4 and 4.27 mg/ml); 50 µl injected volume; Phenogel 40, 50, 60 columns; 1ml/min H_2O with 200 ppm NaN_3 as solvent.

Rheological Detail

Figure S8 demonstrates the absence of a rheological plateau modulus in the measured frequency range for the matrix dextran.

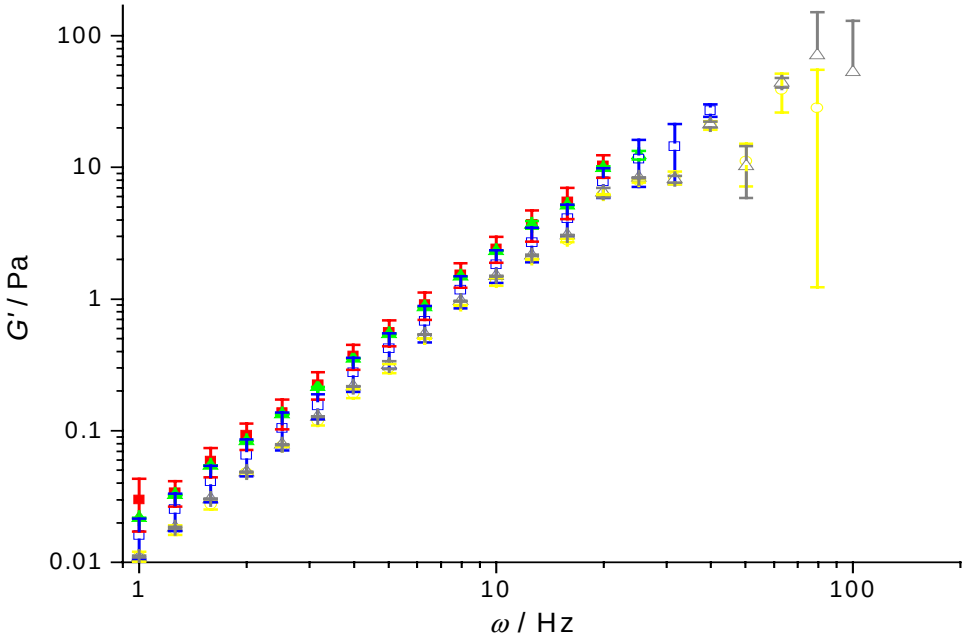

Figure S8. Example of storage modulus, *G′*, as a function of frequencies for different dextran matrix concentrations: w = 5% (■), 10%(▲), 15%(□), 20%(○), and 25%(△)

References

(1) Fong, B.; Stryjewski, W.; Russo, P. S. *J. Coll. Int. Sci.* **2001**, *239*, 374-379.

(2) Baylis, M.; Bu, Z.; Doucet, G. J.; Russo, P. S.; Stryjewski, W.; Temyanko, E.; Tipton, D. L. *J. Chem.l Phys.* **1999**, *111*, 1746-1752.

(3) Bu, Z.; Russo, P. S.; Tipton, D. L.; Negulescu, I. I. *Macromolecules* **1994**, *27*, 6871-6882.

(4) Cush, R. C.; Russo, P. S.; Kucukyavuz, Z.; Bu, Z.; Neau, D.; Shih, D.; Kucukyavuz, S.; Ricks, H. L. *Macromolecules* **1997**, *30*, 4920-4926.

(5) Mustafa, M. B.; Tipton, D.; Russo, P. S. *Macromolecules* **1989**, *22*, 1500-1504.

(6) Bertero, M.; Brianzi, P.; Pike, E. R.; de Villiers, G.; Lan, K. H.; Ostrowski, N. *J. Chem. Phys.* **1985**, *82*, 1551.

(7) Stepanek, P. In *Dynamic Light Scattering, The Method and Some Applications*; Brown, W., ed. Clarendon Press: Oxford, 1993; pp 175-241.